

## **Shear Behavior of RC Beams with Full or Partial SFRC Shear Span**

**Dr. Ali H. Aziz**

Civil Engineering Dept., College of Engineering  
Al-Mustansiriya University, Baghdad, Iraq

**Asst. Lect. Dhia B. Ghailan**

Civil Engineering Dept., College of Engineering  
Al-Mustansiriya University, Baghdad, Iraq

### **Abstract**

*This study presents experimental and theoretical investigation performed to investigate the shear behavior of reinforced concrete beams without shear reinforcement (stirrups) and with full or partial steel fiber reinforced concrete (SFRC) shear span.*

*More rational way has been used by replacing (strengthening) a certain part(s) of shear span by steel fiber reinforced concrete (SFRC). Tests were carried out on four beams, simply supported under single point loading. One of which were made fully with NSC, and the others were made fully or partially with SFRC in shear spans.*

*Experimental results show that the ultimate shear strengths are increased by (17% -150 %), while the reserve shear strength is increased by (18.2 % - 48.8 %) for tested beams strengthened with SFRC, in comparison with the reference beam. Crack arrest mechanism of steel fibers limits crack propagation, improves reserve strength and alters the mode of failure. So, more safety was obtained.*

*ANSYS finite Element package program are used to simulate all tested beams. Three dimensional nonlinear brick element (solid element) was utilized to model the concrete, while, the steel reinforcement was modeled by using a discrete representation (bar element).*

*It was found that the general behavior of the finite element models shows good agreement with the experimental tests results.*

### **الخلاصة**

تقدم هذه الدراسة بحثاً عملياً ونظرياً لتقصي سلوك القص للعتبات الخرسانية المسلحة الخالية من حديد القص (الرباطات) والحاوية كلياً أو جزئياً على خرسانة مسلحة بألياف الحديد (SFRC) في فضاء القص. تم استخدام طريقة أكثر منطقية وذلك ببدال (تقوية) جزء معين من فضاء القص بالخرسانة المسلحة بالألياف الحديد (SFRC). تم فحص اربع عتبات، مسندة اسناداً بسيطاً وتحت تأثير حمل مركز عند المنتصف. احدى العتبات المفحوصة كانت مصنوعة بالكامل من خرسانة اعتيادية المقاومة، اما بقية العتبات فكانت مصنوعة جزئياً أو كلياً من خرسانة مسلحة بالألياف الحديد في مناطق فضاء القص. اظهرت النتائج المختبرية زيادة في مقاومة القص بين (17% - 150%) وزيادة في مقاومة القص المؤمن (Reserve Strength) بين (18.2%-48.8%) للعتبات المقواة بالخرسانة المسلحة بالألياف الحديد، مقارنة مع العتبة المرجعية. لآلية وقف تشقق الألياف الحديدية تحمي من انتشار التشقق، تحسن مقاومة القص وتغير نمط الفشل. لذلك، تم الحصول على نتائج أفضل مع النماذج الرياضية المعتمدة على العناصر المحددة ثلاثية الأبعاد السلاخية لتمثيل الأجزاء الخرسانية وعناصر مفصلة (Discrete Elements) لتمثيل قضبان التسليح. اظهرت النتائج بشكل عام حصول توافق جيد بين نتائج العناصر المحدودة مع النتائج المختبرية.

### **1. Introduction**

Previous researches show that increase in bending moment capacity and shear strength is attainable by using steel fiber reinforced concrete (SFRC) [1,2,3]. This is due to the ability of the steel fibers in arresting crack growth and crack widening (work within crack arrest mechanism). Randomly distributed steel fibers in concrete increase its homogeneous and isotropic characteristics and improve tensile response. Most experimental investigations and researches have suggested replacing the entire normal strength concrete of beams by steel fiber reinforced concrete (fully strengthened by SFRC).

In the present work, a more rational method has been used by replacing (strengthening) the full depth with a certain part(s) of shear span of reinforced concrete beams by steel fiber reinforced concrete.

These replacements (strengthening) may significantly increase shear capacities, reduce costs and "putting each type of concrete into its proper location". As a result, this procedure represents an implicit optimization for strengthening of reinforced concrete beams.

## 2. Experimental Study

### 2-1 Experimental Program

Tests were carried out on four beams, simply supported under single point loading. All beams were singly reinforced concrete (SRC). To ensure the beams to fail in shear mode of failure, the tested beams were made without shear reinforcement (stirrups). The variables were the concrete type of the shear span (ratio of SFRC to NSC length of shear span). The span, section and reinforcement were kept constant for all tested beams.

### 2-2 Specimen Details

Each beam is designated in a way to indicate the shear beam and ratio of SFRC layer in shear span. Thus, specimen (SB-0.75) represents a shear beam, three quarters of its shear span were made from SFRC layer and the rest were made from NSC layer. The tested beams are designated as shown in **Table (1)**.

**Table (1) Properties of test beams**

Beam Designation	Shear Span Concrete***	
	SFRC	NSC
SB-0.0 *	None	a
SB-1.0**	a	None
SB-0.75	$\frac{3}{4}$ a	$\frac{1}{4}$ a
SB-0.50	$\frac{1}{2}$ a	$\frac{1}{2}$ a

\* Reference Beam (Full Beam made with NSC)

\*\* Full Beam made with SFRC

\*\*\* For one side

**Figure (1)** presents the detailed testing program and nominal dimensions of the tested beams. The main reinforcement consisted of ( $2\phi 10\text{mm}$ ) mild, hot-rolled, deformed steel bars employed as tension reinforcement (flexural reinforcement).

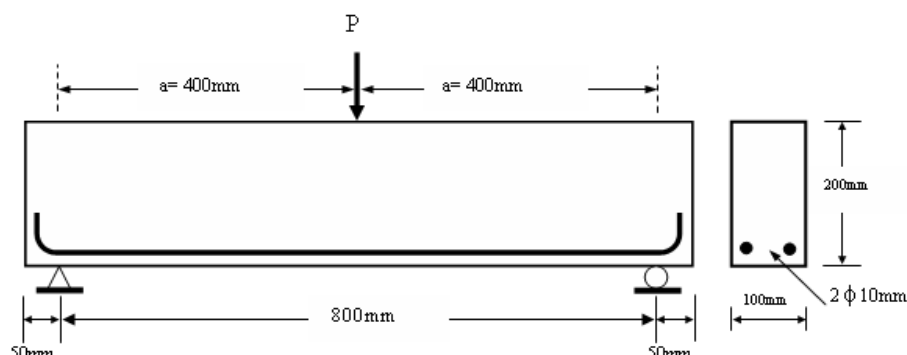


**Figure (1) Details of test beams**

Longitudinal tension reinforcement was bent with ( $90^\circ$ ) angle at the ends to prevent any steel-concrete bond slip. The reinforcement bars were placed inside the mold with (20mm) concrete cover.

### 2-3 Materials

In the experimental program, ( $\phi 10\text{mm}$ ) deformed steel bars having (596.8MPa) yield strength were used as flexural reinforcement (tension reinforcement).

In manufacturing the test specimens, the following materials were used: ordinary Portland cement (Type I); crushed gravel with maximum size of (10mm); natural sand from Al-Ukhaider region with maximum size of (4.75mm) and fineness modulus of (2.84); hooked-end mild carbon steel fibers with average length of (50mm), nominal diameter of (0.5mm), aspect ratio of (100) and yield strength of (1130MPa) (from manufacturers).

The mix proportions for the NSC and SFRC are reported and presented in **Table (2)**.

**Table (2) Proportions of concrete mixes**

Parameter	Concrete Type	
	NSC	SFRC
Water/cement ratio	0.45	0.45
Water ( $\text{kg}/\text{m}^3$ )	202.5	202.5
Cement ( $\text{kg}/\text{m}^3$ )	450	450
Fine Aggregate ( $\text{kg}/\text{m}^3$ )	770	770
Coarse Aggregate ( $\text{kg}/\text{m}^3$ )	900	900
Steel Fiber volume (%)	-	1.0

## 2-4 Test Measurements and Instrumentation

Hydraulic universal testing machine (MFL system) was used to test the beams specimens as well as control specimens. Central deflection has been measured by means of (0.01mm) accuracy dial gauge (ELE type) and (30mm) capacity. The dial gauge was placed underneath the bottom face of the test beam at mid-span.

## 2-5 Test Results of Specimens

Test results of mechanical properties of specimens are summarized in **Table (3)**. Compressive strength for cylinders was carried out on NSC and SFRC in accordance with ASTM-C39 <sup>[4]</sup>. Flexural strength (modulus of rupture) tests were carried out in accordance with ASTM-C78 <sup>[5]</sup>.

**Table (3) Mechanical properties of concrete**

Property (MPa)	Concrete Type	
	NSC	SFRC
Cylinder compressive strength ( $f'_c$ )*	41	44
Modulus of rupture ( $f_r$ )**	4.7	7.5

\*Average of six specimens for each concrete type; using (152x305mm) cylinders.

\*\* Average of six specimens for each concrete type; using (100x100x500mm) prisms.

## 2-6 Test Procedure

All beam specimens were tested using universal testing machine (MFL system) with monotonic loading to ultimate states. The tested beams were simply supported over an effective span of (800mm) and loaded with a single-point load.

The beams have been tested at ages of (28) days. The beam specimens were placed on the testing machine and adjusted so that the centerline, supports, point load and dial gauge were in their correct or best locations.

Loading was applied slowly in successive increments. At the end of each load increment, observations and measurements were recorded for the mid-span deflection and crack development and propagation on the beam surface.

When the beams reached advanced stage of loading, smaller increments were applied until failure, where the load indicator stopped recording any more and the deflections increased very fast without any increase in applied load.

The developments of cracks (crack pattern) were marked with a pencil at each load increment.

### 3. Numerical Study

In order to study more thoroughly the structural behavior of reinforced concrete beams made with full or partial SFRC shear span under the effect of shear and to simulate all tested beams, ANSYS<sup>[6]</sup> finite element program is used.

#### 3-1 Finite Element Model

A nonlinear three dimensional brick element (SOLID-65 in ANSYS) is used to model the concrete (NSC and SFRC). The solid element has eight nodes with three degrees of freedom at each node, translations in the nodal x, y and z-directions. The element is capable of plastic deformation and cracking in three orthogonal directions.

A discrete axial element (LINK-8 in ANSYS) is used to model the steel reinforcement. Two nodes are required for this element; at each node, three degrees of freedom exist identical to those for the brick element.

To avoid stress concentration, (30mm) thick steel plate, modeled by using (SOLID-45 in ANSYS), is added at the support and under the load locations. The element has eight nodes with three degrees of freedom at each node, translations in the nodal x, y and z-directions.

#### 3-2 Materials Properties

##### 3-2-1 Concrete

For the finite element models, compressive uniaxial stress-strain relationship for concrete is described by a multilinear isotropic stress-strain curve. The failure surface is defined by a total of five strength parameters, but it can also be specified by a minimum of two constants ( $f_t$  and  $f'_c$ ) with the other three related as given by **Willam and Warnke** criterion<sup>[7]</sup>. These relations are assumed for both NSC and SFRC.

The shear transfer coefficient ( $\beta_o$ ) for open cracks and ( $\beta_c$ ) for closed cracks, representing conditions of the crack face and determining the amount of shear transferred across the cracks, are used in many studies ranging from (0.0) to (1.0). In this study, for normal strength concrete, ( $\beta_o$ ) and ( $\beta_c$ ) are assumed to be (0.3) and (0.5).

In fiber reinforced concrete, the shear transfer at the cracks depends on the matrix strength and fiber interaction in the fiber pullout mechanism<sup>[8]</sup>. To account for this fact, ( $\beta_o$ ) and ( $\beta_c$ ) are assumed to be (0.35) and (0.6).

In tension, the stress-strain curve for concrete is assumed to be linearly elastic up to the ultimate tensile strength. The tension stiffening of concrete after cracking is represented by providing a linearly descending branch. Smearred cracking approach is utilized to model the cracking of concrete. Poisson's ratio for concrete is assumed to be (0.2) and it is used for all types of concrete. Tensile strength of NSC and SFRC was taken to be equal to the measured modulus of rupture.

The adopted empirical equations of ACI-318<sup>[9]</sup> Committee and the two-phase composite material model (Rule of mixture)<sup>[10]</sup> are used to determine the Modulus of elasticity in the modeling of finite elements, as shown in **Table (4)**.

**Table (4) Modulus of elasticity adopted in finite element analysis**

Concrete Type	Empirical Equation	$f'_c$ (MPa)	$E_c$ (MPa)	Note
NSC	$E_c = 4700\sqrt{f'_c}$	41	30094.7	ACI-318
SFRC	$E_c = E_f V_f + (1 - V_f)E_m$	-	31793.8	Rule of Mixture

### 3-2-2 Steel Reinforcement and Steel Plates

The uniaxial stress-strain relation for steel is idealized as a bilinear curve with Von-Mises yield criterion, representing the elastic-plastic behavior with strain hardening. This relation is assumed to be identical in tension and compression as shown in **Fig.(2)**.

In the present work, the strain hardening modulus ( $E_T$ ) is assumed to be  $(0.03 E_s)$ . This value is selected to avoid convergence problems during iteration.

The steel plates are assumed to be linear elastic materials. An elastic modulus equal to  $(200\text{GPa})$  and Poisson's ratio of  $(0.3)$  are used for the plates and the steel reinforcement.

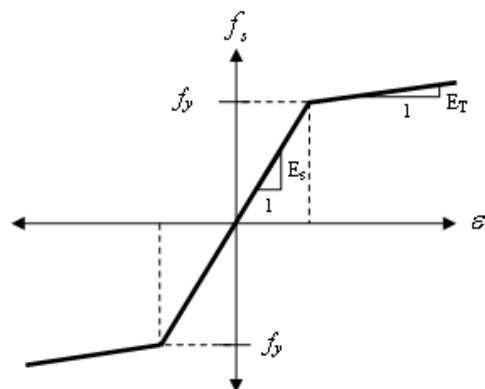


**Figure (2) Modeling of Reinforcing Bars**

### 3-3 Modeling of Beams

The actual dimensions of the tested beams are shown in **Fig.(1)**. By taking advantage of the symmetry of both geometry and loadings, a quarter of the entire beam is used for the finite element modeling, **Fig.(3)**.

The origin point of coordinates coincides with the center of the cross-section for the concrete beam. Due to symmetry, only one loading plate and one support plate are needed. As an initial step, the beams, plates and supports were modeled as volumes (solid elements).

Casting was continuous and accordingly no construction joints occurred between the different layers. Thus, no interface elements were needed in the finite element analysis.

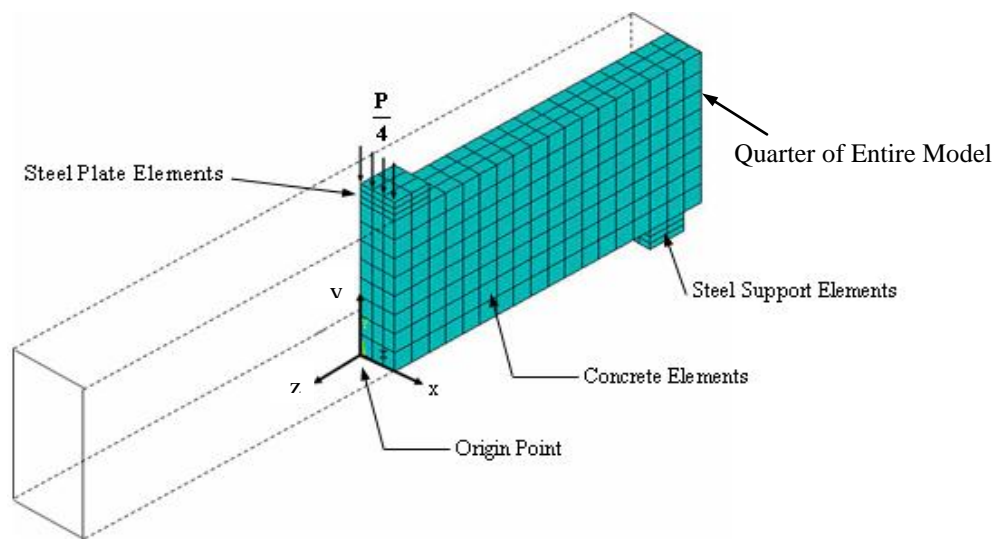


**Figure (3) Mesh of the concrete, loading steel plate, and steel support**

### 3-3-1 Meshing

After specifying the volumes, a finite element analysis requires meshing of the model. In other words, the model was divided into a number of small elements, and after loading, stresses and strains were calculated at integration points of these small elements. To obtain good results, the mesh was set up such that square or rectangular elements were created, **Fig.(3)**.

Due to load concentration by applied load directly on concrete elements, in the early attempt (before spreading the load by using steel plates), crushing of the concrete started to develop in elements located directly under loads. Subsequently, adjacent concrete elements crushed within few load steps. As a result, the model showed a large displacement, the solution diverged and finally, the finite element model failed prematurely. Therefore, to prevent this premature failure phenomenon, steel plates were used under load and at beam supports.

### 3-3-2 Loads and Boundary Conditions

Displacement boundary conditions are needed to constrain the model for obtaining a unique solution. To ensure that the model acts the same way as the experimental beams boundary conditions need to be applied at points of symmetry, and where the supports and loadings exist. This approach reduced computational time and computer disk space requirements.

Planes of symmetry are required at the internal faces. At the plane of symmetry, the displacement in the direction perpendicular to that plane is held zero (roller). The

displacements in the plane of symmetry were constrained by providing rollers along the axes of symmetry.

The external load was applied on a steel plate across the entire centerline of the plate; thus, the external applied load was represented by the equivalent nodal forces on the top nodes of the same place of plate. Therefore, the equivalent force at each node on the plate was ( $\frac{P}{16}$ ) of the actual force applied. The steel plate had four edge nodes, thus ( $\frac{P}{4}$ ) is divided into four ( $\frac{P}{16}$ ) (simple lumping).

The application of the loads up to failure was done incrementally as required by the Newton-Raphson procedure. Therefore, the total applied load was divided into a series of load increments (load steps). Within each load step, maximum of (50) iterations were permitted.

At certain stages in the analysis, load step size was varied from large (at points of linearity in the response) to small (when cracking and steel yielding started). In all cases, convergence was achieved before reaching the maximum (50) iteration.

Failure for each of the models is defined when the solution for a minimum load increment still does not converge (convergence fails). The program then gives a message specifying that the models have a significantly large deflection (rigid body motion).

## 4. Results and Discussion

As mentioned before, the main objectives of this study are to examine or assess the effect of steel fiber reinforced concrete (in shear span) on shear behavior of reinforced concrete beams.

During the experimental work, cracked and ultimate loads, load versus deflection at mid-span were recorded. Photographs for the tested beams were taken to show the crack pattern and some other details.

The recorded data, general behavior and test observations are reported as well as recognizing the effects of various parameters on the shear behavior.

Verification is carried out in order to check the validity and accuracy of the finite element procedure. The accuracy of the finite element models is determined by ensuring that failure modes are correct and the ultimate load is reasonably predicted in comparison with the experimental results.

### 4-1 Experimental Results

#### 4-1-1 General Behavior

Photographs of the tested beams are shown in **Fig.(4)** and test results are given in **Table (5)**. All beams are designed to fail in shear. The general behavior of the tested beams can be described as follows:



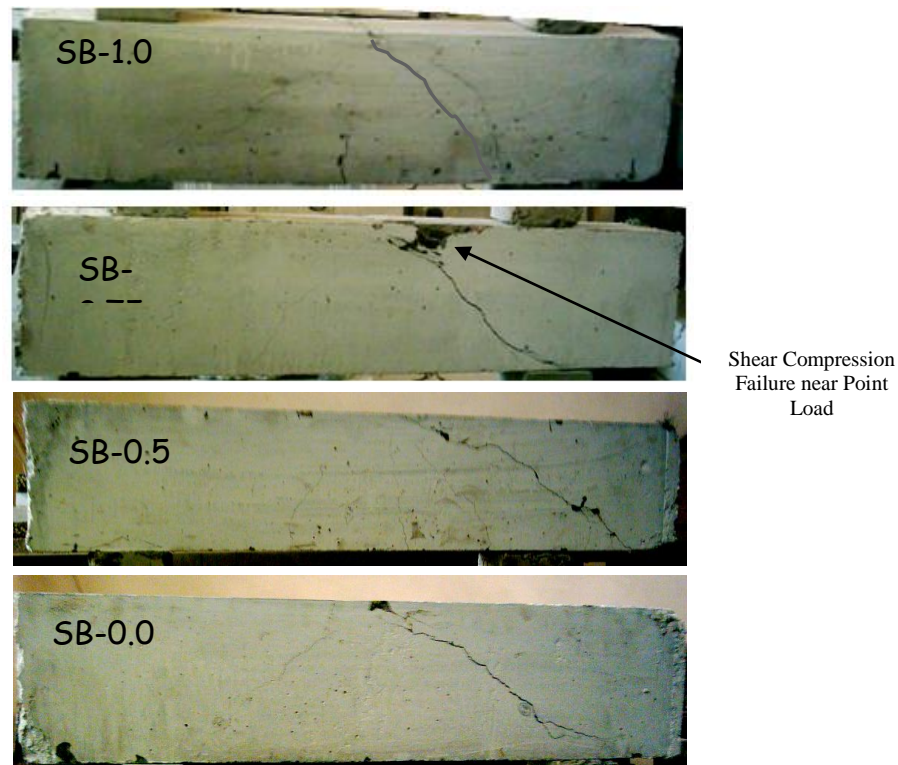


**Figure (4) Crack pattern for tested beams**

At early stage of loading, flexural cracks were observed first in the mid-span region. As the load increased, the flexural cracks spread into the shear span. Some of these cracks gradually increased in depth and began to incline towards the applied loads. Since all the beams failed in shear, final failure took place by opening up of one of the diagonal cracks over the entire depth, and then crushing failure occurred in the concrete near the compression face at the point load. This mode of failure indicated a diagonal crack with shear compression mode, as shown in **Fig.(4)**. A diagonal crack is defined as a major inclined crack extending from the level of the longitudinal reinforcement to the region of point load <sup>[11]</sup>.

The primary difference between the observed cracking patterns was the angle at which the primary shear crack was formed. The crack inclination observed in beam (SB-0.0) was steeper than that observed in beams which had fully or partially SFRC in shear span. This means that the steel fibers can act like shear reinforcement like small diameter bars, when the fibers are closely spaced and randomly distributed.

#### **4-1-2 Failure Mode**

In the experimental work, the failure modes for the beams were as predicted. The mode of failure was typical of shear-compression failure. This mode of failure took place due to crushing in the concrete near the compression zone (face) at the point load <sup>[12]</sup>. The failure modes for all of the tested beams are reported in **Table (5)**.

Table (5) Failure mode and reserve shear strength

Beam Designation	Experimental		% Reserve Shear*	Failure Mode
	V <sub>u</sub> (kN)	V <sub>cr</sub> (kN)		
SB-0.0	24	22	9.1	Shear Compression
SB-1.0	60	38	57.9	Shear Compression
SB-0.75	45	30	50	Shear Compression
SB-0.50	28	22	27.3	Shear Compression

$$* \text{ Reserve Shear} = \left( \frac{V_u - V_{cr}}{V_{cr}} \right) * 100$$

The inclined cracks formed suddenly then extended along the shear span (from the beam support upwards to the point load) and causing the beam to fail instantaneously (for the beam SB-0.0) along a single shear crack.

In beam (SB-0.0), which had no steel fibers, the diagonal cracks were wide and tended to branch off, whereas in other beams which had fully or partially SFRC in shear span, the diagonal crack was narrower. Randomly distributed steel fibers in the shear span were effective after the formation of cracks and continued to resist significant tension until the fibers yielded or pulled out.

#### 4-1-3 Reserve Shear Strength

Shear forces corresponding to a diagonal tension cracking ( $V_{cr}$ ) and failure ( $V_u$ ) are given in **Table (5)** in addition to the percentage reserve shear strength for all tested beams.

The reserve shear strength, which is defined as the ratio of the difference of ultimate load and diagonal cracking load to the diagonal cracking load <sup>[1]</sup>, is a measure of the reserve strength beyond diagonal cracking. The percentage of reserve shear strengths were (9.1%, 57.9%, 50% and 27.3%) for the tested beams (SB-0.0, SB-1.0, SB-0.75 and SB-0.5) respectively.

The tested beams (SB-1.0) and (SB-0.75) had the greater values, this is due to the larger crack arrest mechanism of steel fibers which improves better the tensile response, and limits the crack propagation, thus improving the reserve strength of these beams.

The reserve shear strength of the tested beam (SB-0.5) was approximately equal to half of that in (SB-1.0), this means that the reserve shear strength is proportional with the SFRC in shear span.

For beam (SB-0.0), marginal value of reserve shear strength were obtained, this may be due to the absence of SFRC in shear span.

Generally, all beams which had SFRC occupying fully and partially the shear span exhibited better reserve shear strength.

#### 4-1-4 Ultimate Shear Strength

The ultimate shear strength of the tested beams was compared with the reference (control) beam, (SB-0.0), and reported in **Table (6)** in terms of shear force at failure ( $V_u$ ).

The shear strength of the tested beams (SB-1.0), (SB-0.75) and (SB-0.5), with full or partial occupation of SFRC in the shear span, was increased (150%, 88% and 17%) respectively. Presence of steel fibers spanning the micro-cracks controlled the crack propagation and the rate of widening of cracks, which ultimately led to a higher load carrying capacity.

Marginal value of shear strength of the tested beam (SB-0.5) means that the used ratio of SFRC in shear span (i.e., 0.5a) did not affect to increase the shear strength considerably.

**Table (6) Ultimate load capacity**

Beam Designation	Experimental	
	$V_u$ (kN)	$(V_u)_i / (V_u)_R$
SB-0.0	24	1.0
SB-1.0	60	2.5
SB-0.75	45	1.88
SB-0.50	28	1.17

\* $(V_u)_i$  = Ultimate shear capacity of Considered Beam

\*\* $(V_u)_R$  = Ultimate shear capacity of Reference Beam, (SB-0.0)= 24 kN.

#### 4-1-5 Load-Deflection Response

Deflections were measured at mid-span at the center of the bottom face of the beams. **Fig.(5)** shows the load deflection plots for the experimentally tested beams.

By observing the load-deflection characteristics of the tested beams, it is seen that the ductility of the beams increased when the concrete of the shear span changed from normal strength concrete (without steel fibers) to full SFRC

The ductility of beam specimen (SB-1.0) was better when compared to those of (SB-0.0) and (SB-0.5). Presence of SFRC increased both the load carrying capacity and the ultimate deflection, which is defined as the deflection at which the load resistance drops significantly. Here, ductility is measured as the ratio of deflection at ultimate load to the deflection at first cracking or yielding.

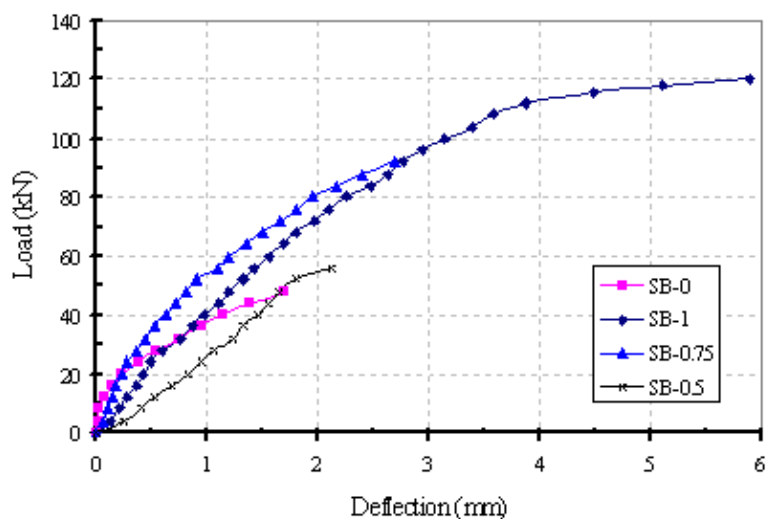


Figure (5) Load deflection relationship for tested beams

## 4-2 Numerical Results

### 4-2-1 Ultimate Shear Capacity

Table (7) shows comparisons between the ultimate shear of the experimental beams and the final loads from the finite element models. The final loads from the finite element models are the last applied load steps before the solution diverges.

The numerical model predicted an ultimate shear strength of (28kN), (58.2kN), (48kN) and (32kN) for beams (SB-0.0), (SB-1.0), (SB-0.75) and (SB-0.5) respectively and captured well the shear mode of failure.

When comparing with the experimental values, the numerical models showed (17%), (7%) and (14%) higher ultimate loads for the beams (SB-0.0), (SB-0.75) and (SB-0.5) respectively. While, the numerical model of the beam (SB-1.0) showed lower in ultimate strength by about (3%).

Table (7) Ultimate shear strength

Beam Designation	Ultimate shear strength (kN)		% $\frac{(V_u)_{FEM}}{(V_u)_{EXP.}}$
	$(V_u)_{EXP.}$	$(V_u)_{FEM.}$	
SB-0.0	24	28	1.17
SB-1.0	60	58.2	0.97
SB-0.75	45	48	1.07
SB-0.50	28	32	1.14

#### 4-2-2 Crack Patterns

ANSYS program records a crack pattern at each applied load step. Crack patterns obtained from the finite element analyses and from the failure modes of the experimental beams agree well, as shown in **Fig.(6)**.

The appearance of the cracks reflects the failure mode of the beams. The finite element model accurately predicts that the beams fail in shear and predicts that diagonal cracks are formed diagonally and move up towards the load location.

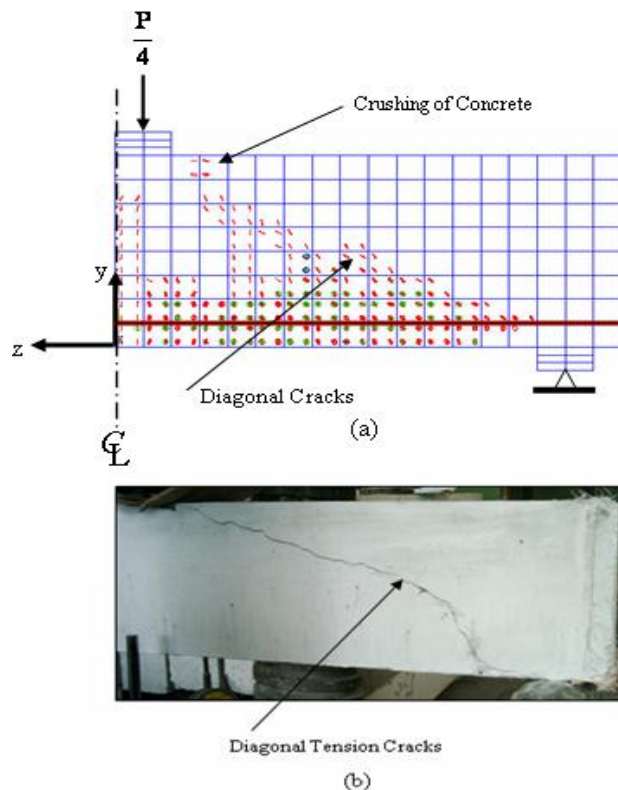


**Figure (6) Crack patterns for shear beams:**  
**(a) crack pattern from FE model**  
**(b) crack pattern of experimentally tested beams**

#### 5. Conclusions

Based on the results obtained by the experimental work and the finite element analysis for the reinforced concrete beams made without shear reinforcement (stirrups), with full and partial steel fiber reinforced concrete (SFRC) shear span, the following conclusions are presented:

1. The shear strength of the tested beams (SB-1.0), (SB-0.75) and (SB-0.5), with SFRC occupying fully or partially the shear span was increased (150%, 88% and 17%) respectively. Presence of steel fibers spanning the micro-cracks controlled the crack propagation and the rate of widening of cracks, which ultimately led to a higher load carrying capacity.

2. Shear strength of tested beam (SB-0.5) was marginal, this means that the used ratio of SFRC in shear span (i e.,  $0.5a$ ) did not affect significantly to increase the shear strength. Also, this means the effective zone to resist shear stresses lies between three fourth to entire shear span (for single-point load test).
3. All beams which had SFRC occupying fully or partially the shear span exhibited good reserve shear strength. The reserve shear strength was proportional with the SFRC in the shear span. The percentages of reserve shear strength were (9.1%, 57.9%, 50% and 27.3%) for the tested beams (SB-0.0, SB-1.0, SB-0.75 and SB-0.5) respectively.
4. The crack inclination observed in beam (SB-0.0) was steeper than that observed in beams which had SFRC in shear span. This means that the steel fibers act like shear reinforcement like small diameter bars, when the fibers are closely spaced and randomly distributed.
5. The failure mechanism of the reinforced concrete beam was modeled quite well by the finite elements, and the failure loads predicted were very close to the failure loads obtained from the experimental testing. The general behavior by the finite element models showed good agreement with the test data from the experimentally tested beams. The crack patterns at the final loads from the finite element models corresponded well with the observed failure modes of the experimental beams.

## 6. References

1. Shah, R. H., and Mishra, S. V., "***Crack and Deformation Characteristics of SFRC Deep Beams***", Journal of Indian Engineering, Vol. 85, May 2004, pp. 44-48.
2. Noghabai, K., "***Beams of Fibrous Concrete in Shear and Bending: Experimental and Model***", ASCE-Journal of Structural Engineering, Vol. 126, No. 2, February 2000, pp. 243-251.
3. Gustafsson, J., and Noghabai, K., "***Steel Fibers as Shear Reinforcement in High Strength Concrete Beams***", Lulea University of Technology, Division of Structural Engineering, Stockholm, Sweden, 2005, (Web Site).
4. ASTM, "***Test Method for Compressive Strength of Cylindrical Concrete Specimens***", ASTM C39-96, American Society for Testing and Materials, 1996.
5. ASTM, "***Standard Test Method for Flexural Strength of Concrete (Using Simple Beam with Third-Point Loading)***", ASTM C78-75, American Society for Testing and Materials, 1975.
6. "***ANSYS Manual***", Version (7.0), USA, 2002.
7. Willam, K., and Warnke, E., "***Constitutive Model for the Triaxial Behavior of Concrete***", Proceedings, International Association for Bridge and Structural Engineering, Vol. 19, ISMES, pp. 174, Bergamo, Italy, 1975, [Cited by Ref. (6)].

8. Thomas, J., and Ramaswamy, A., “*Finite Element Analysis of Shear Critical Prestressed SFRC Beams*”, Computer and Concrete, Vol. 3, No. 1, 2006, pp. 65-77.
9. ACI Committee 318, “*Building Code Requirements for Structural Concrete (ACI 318- M 95)*”, American Concrete Institute, Detroit, USA.
10. Raouf, Z. A., and Hussain, A. A., “*Technical notes: Some Properties of Steel Fiber Concrete at Early Ages*”, International Journal of Cement Composites and Lightweight Concrete, Vol. 6, No. 2, May-1984, pp. 117-121.
11. Sethunarayanan, R., “*Ultimate Strength of Pre-tensioned I-beams in Combined Bending and Shear*”, Magazine of Concrete Research, Vol. 12, No. 35, July 1960, pp. 83-90.
12. Wang, C. K., and Salmon, C. G., “*Reinforced Concrete Design*”, 4<sup>th</sup> Edition, Harper International Edition, New York, 1985, 947 p.

### **Notation and Abbreviations**

$a =$	shear Span
$D_f =$	steel fiber diameter;
$E_c =$	modulus of elasticity of concrete;
$E_f =$	modulus of elasticity of steel fiber;
$E_m =$	modulus of elasticity of plain concrete (matrix) within fibers;
$E_s =$	modulus of elasticity of steel;
$E_T =$	tangent modulus of elasticity of steel;
$f'_c =$	cylinder compressive strength of concrete;
$f_r =$	flexural strength of concrete (modulus of rupture);
$f_s =$	steel stress;
$f_y =$	yield strength of steel;
$L_f =$	steel fiber length;
$V_f =$	steel fiber volume fraction;
$V_{cr} =$	diagonal cracking load;
$V_u =$	ultimate shear strength;
$(V_u)_{EXP.} =$	ultimate shear strength obtained from experimental tests;
$(V_u)_{FEM.} =$	ultimate shear strength obtained from finite element analysis.
$\beta_o =$	shear transfer coefficient for open cracks;
$\beta_c =$	shear transfer coefficient for closed cracks;
$\epsilon_s =$	steel strain;

$\phi$ =	<i>diameter of reinforcement bar;</i>
ACI=	<i>American Concrete Institute</i>
ASTM=	<i>American Society for Testing and Materials</i>
ANSYS=	<i>Analysis System Program (package)</i>
F.E.M=	<i>Finite Element Method</i>
NSC=	<i>Normal Strength Concrete</i>
SFRC=	<i>Steel Fiber Reinforced Concrete</i>